

Photoluminescence dynamics and Auger fountain in three-dimensional Si/SiGe multilayer nanostructures

E.-K. Lee,¹ D. J. Lockwood,² J.-M. Baribeau,² A. M. Bratkovsky,³ T. I. Kamins,³ and L. Tsybeskov¹

¹*Department of Electrical and Computer Engineering, New Jersey Institute of Technology, Newark, New Jersey 07102, USA*

²*Institute for Microstructural Sciences, National Research Council, Ottawa, Ontario, Canada K1A 0R6*

³*Hewlett-Packard Laboratories, Palo Alto, California 94304, USA*

(Received 21 May 2009; published 22 June 2009)

In three-dimensional cluster morphology multilayer Si/SiGe nanostructures, we find an anticorrelation between photoluminescence (PL) originating from SiGe clusters and the PL associated with electron-hole droplets (EHDs) localized within nanometer-thick Si separating layers. We show that Auger processes eject holes from SiGe clusters and facilitate the exciton/EHD phase transition in the Si layers. An unusual *N*-shaped SiGe cluster PL decay curve is attributed to the reverse EHD/electron-hole gas phase transition and carrier redistribution between Si spacer layers and SiGe clusters.

DOI: [10.1103/PhysRevB.79.233307](https://doi.org/10.1103/PhysRevB.79.233307)

PACS number(s): 78.55.Qr, 71.35.Ee, 78.47.Cd, 78.67.Bf

The practical application of photoluminescence (PL) in three-dimensional (3D) cluster morphology multilayer Si/SiGe nanostructures with an emission wavelength in the range of 1.3–1.6 μm and exhibiting a quantum efficiency of up to 1% at low excitation intensity is severely limited by the PL intensity saturation under increasing excitation.^{1–3} An explanation of this phenomenon involving enhanced nonradiative Auger processes in Si/SiGe nanostructures has been proposed.^{4–6} It has also been suggested that the suspected type II energy band alignment at the Si/SiGe heterointerface⁷ is responsible for the recently reported very long (up to 10^{-2} s) carrier radiative lifetime.⁵ The combination of the enhanced Auger processes, very low density of structural defects,² and extremely slow radiative recombination⁵ could make a 3D Si/SiGe nanostructure an ideal “Auger fountain” emitter, a system where Auger recombination ejects carriers from the energy wells into the energy barriers.⁸ In contrast to the traditional view of Auger recombination as a strictly nonradiative process, the Auger fountain is found to be responsible for efficient carrier transfer and luminescence upconversion, which has so far been observed only in III-V heterostructures and nanostructures.^{8,9} It has also been predicted that this process is enhanced by a relaxation of the momentum conservation selection rules and suggested that low or even threshold-less Auger recombination channels can be established.^{10,11} In this Brief Report, we demonstrate this effect in Si/SiGe 3D nanostructures where Si energy barriers and SiGe cluster energy wells in the valence band form a coupled electronic system. In this system, carrier recombination in the Si spacer layers is directly mediated by Auger processes in the SiGe nanoclusters. In contrast to III-V semiconductors with their intrinsically short carrier radiative lifetimes, the much longer lifetime in Si leads to a nonlinear process involving exciton condensation in the Si barriers and an Auger-mediated exciton/electron-hole droplet (EHD) phase transition, which controls the interplay between Si and SiGe PL bands.

The samples were grown by molecular beam epitaxy in a VG Semicon V80 system. The structures, grown on (001) Si at temperature $T_G=650$ °C, consist of 10-period Si/Si_{1-x}Ge_x multiple layers with $x\approx 0.55$ close to the center of each SiGe

cluster. Transmission electron microscopy (TEM) studies have shown that the Si/Si_{1-x}Ge_x multilayers exhibit an islandlike morphology (i.e., 3D growth) embedded into a Si matrix (Fig. 1, inset; see also Ref. 12 for more details). The Si_{1-x}Ge_x island height and Si separating layer thickness were kept constant throughout the entire multilayer structure. The PL measurements were performed using a closed-cycle vacuum cryostat in the temperature range of 15–300 K. For continuous wave (CW) PL measurements, we used an argon ion laser (476.5 nm) with the excitation intensity varied from 0.1 to 10 W/cm². The PL signal was dispersed using a single grating Acton Research 0.5 m monochromator and

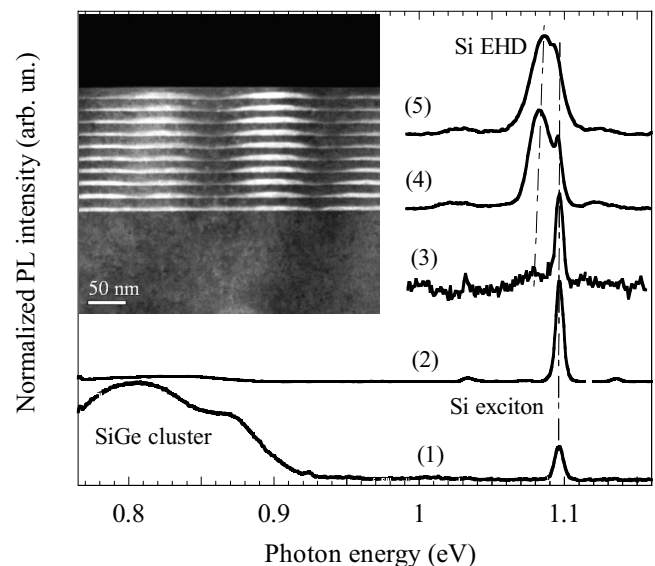


FIG. 1. The PL spectra in 3D Si/SiGe nanostructures measured under CW excitation with intensities of (1) ~ 1 W/cm² and (2) ~ 100 W/cm²; and under pulsed excitation with 6 ns pulse duration and energy densities of (3) $\sim 10^{-5}$ J/cm², (4) $\sim 10^{-3}$ J/cm², and (5) $\sim 10^{-2}$ J/cm². The PL spectra are shifted vertically for clarity and PL peaks associated with SiGe clusters, Si free excitons, and Si EHDs are indicated. The inset shows a dark-field cross-sectional TEM micrograph with SiGe clusters as lighter areas separated by ~ 10 – 15 nm-thick Si layers.

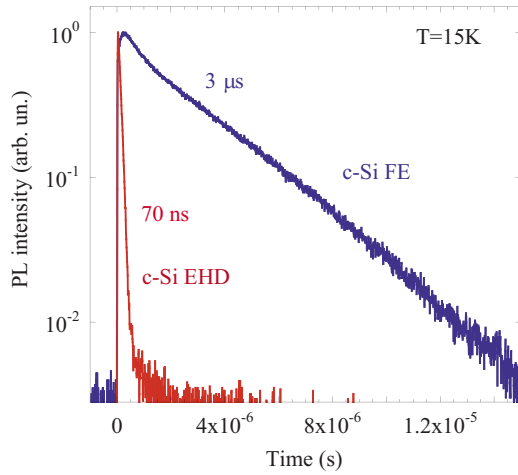


FIG. 2. (Color online) Low-temperature PL dynamics in a controlled ($\rho \geq 10^4 \Omega \text{ cm}$) bulk *c*-Si sample under 0.1 mJ/cm^2 energy density excitation recorded at photon energies associated with the Si free exciton ($\sim 1.096 \text{ eV}$) and Si EHD ($\sim 1.079 \text{ eV}$) PL bands.

detected by a cooled Hamamatsu photomultiplier in the spectral range of $0.9\text{--}1.6 \mu\text{m}$ ($0.77\text{--}1.38 \text{ eV}$). For PL measurements under pulsed laser excitation, the second harmonic of a Nd:YAG laser with a wavelength of 532 nm , a 6 ns pulse duration, and a known pulse energy density was used. The time-resolved PL signal was stored in a LeCroy digital storage oscilloscope. The overall time resolution of the entire system was $\sim 2 \text{ ns}$.

Figure 1 shows PL spectra measured under different levels of photoexcitations. Using relatively low ($\leq 1 \text{ W/cm}^2$) CW excitation, we observe a broad PL feature in the range of $0.75\text{--}0.9 \text{ eV}$ associated with SiGe clusters and a much weaker PL peak associated with Si exciton recombination at 1.096 eV . On increasing the excitation intensity we find, in agreement with Refs. 2–4, a rapid saturation of the SiGe cluster PL. Under pulsed excitation with the duration of $\sim 6 \text{ ns}$ and energy density of $\sim 0.1 \text{ mJ/cm}^2$, which corresponds to nearly $\sim 1,000$ times higher peak intensity, SiGe cluster PL becomes negligible compared to Si PL. At the same time, a broader PL peak at 1.079 eV appears. With the excitation intensity approaching 10 mJ/cm^2 , this broad PL peak shifts to a slightly higher photon energy ($\sim 1.085 \text{ eV}$), and it quickly becomes the dominant PL feature (Fig. 1). We find that the intensity of this PL band as a function of excitation intensity follows the dependence $I_{\text{PL}} \sim I_{\text{exc}}^n$, with $n \approx 1.2\text{--}2$, and it anticorrelates with SiGe cluster PL where n correspondingly varies from 0.8 to 0.5 . This faster growing, broader PL band is associated with the recombination of Si electron-hole condensates or EHDs.^{13–15}

Figure 2 shows low-temperature PL dynamics in a controlled high resistivity ($\geq 10^4 \Omega \text{ cm}$) bulk *c*-Si sample and focuses on Si exciton recombination at 1.096 eV and Si EHD recombination at 1.079 eV . We find a dramatic difference in the PL decay lifetimes, changing from $\sim 3 \mu\text{s}$ in Si exciton PL to $\sim 70 \text{ ns}$ in Si EHD PL. Under the applied excitation intensity, both PL decays are nearly single exponential. The PL rise time in *c*-Si EHDs is faster than our time resolution, while in *c*-Si exciton PL the rise time is $\sim 20 \text{ ns}$.

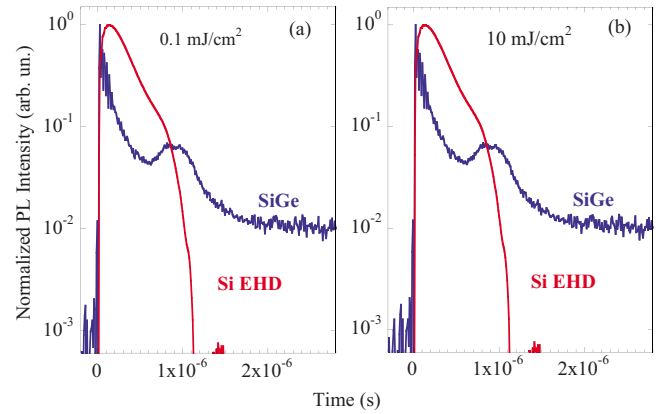


FIG. 3. (Color online) The PL dynamics under pulsed laser energy densities of (a) 0.1 and (b) 10 mJ/cm^2 recorded at photon energies associated with SiGe cluster PL ($\sim 0.82 \text{ eV}$) and Si EHD PL ($\sim 1.08 \text{ eV}$).

Figure 3 depicts low-temperature PL dynamics in 3D Si/SiGe nanostructures, focusing on SiGe cluster PL (measured at a photon energy of 0.82 eV) and Si EHD PL with a peak at $\sim 1.08 \text{ eV}$. The PL associated with SiGe clusters rises practically instantaneously, while the PL associated with Si EHDs, in contrast to that in bulk *c*-Si (Fig. 2), has a slower rise time of $\sim 20\text{--}40 \text{ ns}$. Under an excitation energy density of 0.1 mJ/cm^2 , the SiGe cluster PL decay is nonexponential, with a fast initial characteristic lifetime of $\sim 20 \text{ ns}$ followed by a much slower ($\tau \geq 10^{-4} \text{ s}$) decaying PL. At the same time, the Si EHD PL has a nearly single exponential decay with a lifetime $\tau_{\text{EHD}} \sim 50 \text{ ns}$ [Fig. 3(a)]. Using a 100 times higher excitation intensity, we find an acceleration of the fast component of SiGe cluster PL decay surprisingly followed by a nonmonotonic, at first rising and then falling (i.e., *N*-shape) PL signal [Fig. 3(b)]. Under the same excitation conditions, the Si EHD PL exhibits a nearly exponential decay with a lifetime of $\sim 200 \text{ ns}$ followed by a very fast (faster than 20 ns) decay [Fig. 3(b)]. The Si exciton PL dynamics in Si/SiGe 3D nanostructures, similar to that in bulk *c*-Si, is much slower, with a microsecond characteristic lifetime (not shown).

Assuming the previously suggested quasi-type-II energy band alignment at Si/SiGe heterointerfaces (see Ref. 7), we propose that a 3D Si/SiGe nanostructure can be represented by a coupled electronic system, where Auger recombination in SiGe clusters is not only responsible for fast saturation of the SiGe cluster PL intensity but also injects “Auger holes” into the Si nanometer-thick layers. This process facilitates the formation of Si EHDs. Thus, compared to bulk *c*-Si, where at an excitation energy density of $\geq 0.1 \text{ mJ/cm}^2$ EHDs are formed practically instantly from hot electron-hole plasma condensation,¹⁴ in Si/SiGe 3D nanostructures Si EHD formation is mediated by the Auger processes with a characteristic time of $\sim 10^{-8} \text{ s}$.

At first glance, the proposed luminescence mechanism is qualitatively similar to the previously reported “Auger fountain” in III-V heterostructures with type II energy band alignment.^{8,9} However, in 3D Si/SiGe nanostructures, Auger-excited holes and photogenerated electrons recombine within

the nanometer-thick Si layers, and Si is known to be the classic example of an indirect band gap semiconductor with slow carrier radiative recombination ($\tau_{\text{Si}}^{\text{radiative}} \sim 10^{-3}$ s) and a low PL quantum efficiency.^{15,16} Why, then, can we observe the Si EHD luminescence with a superlinear excitation intensity dependence and a nanosecond lifetime?

Our explanation is based on the qualitative difference between recombination conditions in the nanometer-thick Si layer under low and high levels of photoexcitation. In pure Si, at low excitation intensity and low temperature, an electron-hole pair forms an exciton, and its radiative lifetime is long due to the low probability of a three particle (electron-hole-phonon) process.¹⁷ At high photogenerated carrier density, the recombination conditions change drastically, mainly due to the formation of EHDs. Compared to free exciton PL, the EHD PL peak photon energy is reduced due to strong carrier-carrier interactions.¹⁸ More importantly, the electron-phonon interaction increases the local lattice temperature and produces additional nonequilibrium phonons with energy-momentum dispersion quite different compared to that at thermal equilibrium.^{18–21} The probability of phonon-assisted transitions in a system with a significantly disturbed (or “whitened”) phonon spectrum increases, and carrier lifetime drops down to $\sim 10^{-7}$ s (Figs. 2 and 3). Thus, in a low defect density environment (i.e., low concentration of nonradiative recombination centers), Si EHD radiative recombination may become the dominant recombination channel. It is important in this respect that in Si nanostructures (e.g., ultrathin silicon-on-insulator, Si/SiGe quantum wells, etc.) the threshold for EHD formation is much lower compared to that in bulk Si because of the system-reduced dimensionality and suppressed carrier diffusion.^{22,23} Also, in bulk Si, the EHD typical size is in the range of $\sim 10^{-4}$ cm, and its evolution is governed by many phenomena including EHD surface tension, boundaries between the EHD and the exciton gas, EHD deformation, diffusion, evaporation, etc. (see Ref. 24). For example, under increasing excitation intensity, the size of the Si EHD increases, and the Si EHD PL lifetime increases as well, similar to that shown in Fig. 3. However, many of these processes could be quite different in ~ 10 -nm-thick Si layers and will be discussed elsewhere.

The proposed recombination mechanism is summarized in Fig. 4. At low excitation intensity [Fig. 4(a)], the Si electron-hole density is too low for EHD condensation and Si carrier recombination is slow. Under these conditions, photogenerated holes created in Si would rather fall into SiGe clusters. Thus, assuming a defect-free Si/SiGe heterointerface, slow radiative recombination between spatially separated electrons and holes at the Si/SiGe heterointerface is the only possible channel of radiative recombination. This conclusion is supported by the spectra given in Fig. 1, which show a dominant SiGe PL band only at low excitation intensity.

At a high level of photoexcitation [Fig. 4(b)], SiGe Auger recombination overcomes the slow recombination of spatially separated electrons and holes at the Si/SiGe heterointerface (i.e., an indirect exciton). This process generates “Auger holes” with energies in the range of 0.7–0.8 eV, while the valence energy barrier at the Si/SiGe heterointerface is < 0.3 – 0.4 eV, and thus the fast Auger hole injection from

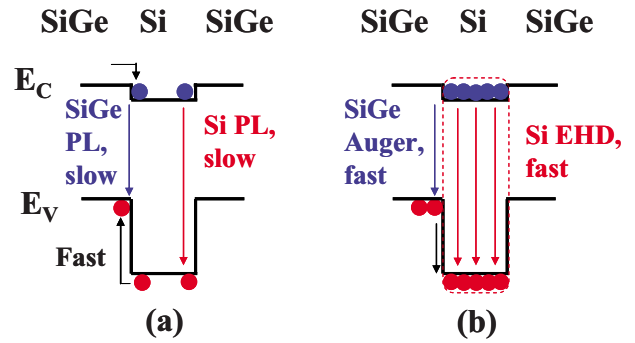


FIG. 4. (Color online) Schematic representation of recombination processes in a Si/SiGe 3D nanostructure. (a) At low excitation intensity, because of the long carrier radiative lifetime in Si energy barriers, a hole falls into a SiGe energy well and recombines with an electron localized in Si. (b) At high excitation intensity, the “Auger fountain” ejects holes from SiGe clusters into Si layers and facilitates the formation of Si EHDs. The fast Si EHD recombination becomes the dominant recombination mechanism.

SiGe clusters into Si barriers can be very efficient.^{10,11} The Auger-mediated hole transfer from SiGe clusters into Si barriers not only suppresses the SiGe cluster PL but also contributes to carrier accumulation in the nanometer-thick Si separating layers resulting in EHD condensation. According to our measurements, the Si EHD lifetime is less than 10^{-7} s, and at high excitation intensity this is the dominant recombination channel.

The EHD condensation from the electron-hole gas is a first-order phase transition, and it depends on the excess carrier concentration and temperature.^{12,13} According to our data [Fig. 3(b)], it takes $\sim 10^{-6}$ s after the short (6×10^{-9} s) laser pulse for the carrier concentration to drop below the EHD condensation threshold and for the reverse EHD/electron-hole gas phase transition to take place. This reverse phase transition creates recombination conditions very similar to that at low excitation intensity. Thus, instead of waiting a long time to recombine with an electron, a hole located in the Si barrier would be quickly recaptured by the SiGe cluster, where it will eventually recombine with an electron in Si [Fig. 4(a)]. This hole capture by SiGe energy wells explains the observed rise (after $\sim 10^{-6}$ s) in the SiGe PL intensity [Fig. 3(b)]. The longer time ($> 10^{-6}$ s) part of the SiGe PL decay is governed by the continuously decreasing SiGe cluster carrier concentration.

In conclusion, we have shown that in 3D Si/SiGe nanostructures Auger recombination is not only responsible for the quick saturation of the SiGe cluster PL intensity as a function of excitation intensity but it also effectively injects holes into the Si barriers. This hole Auger fountain, presumably enhanced by the relaxation of the momentum conservation selection rules at the Si/SiGe heterointerface, facilitates the efficient formation of EHDs and an exciton/EHD phase transition in the nanometer-thick Si layers. We have also shown that at excitation energy densities of 10^{-5} – 10^{-2} J/cm², Si EHD recombination becomes the dominant channel of radiative recombination. The same mechanism explains the experimentally observed anomalies in the PL dynamics and indicates that the reverse EHD/

exciton phase transition is responsible for the nonmonotonic, *N*-shaped SiGe cluster PL decay. This phase transition in nanometer-thick Si layers could lead to novel low-threshold nonlinear optical phenomena in 3D Si/SiGe nanostructures.

We thank X. Wu for the TEM micrograph shown in Fig. 1. The work at the New Jersey Institute of Technology has been supported in part by Intel Foundation at NJIT and the U.S. National Science Foundation.

-
- ¹L. C. Lenchyshyn, M. L. W. Thewalt, D. C. Houghton, J.-P. Noël, N. L. Rowell, J. C. Sturm, and X. Xiao, *Phys. Rev. B* **47**, 16655 (1993).
- ²B. V. Kamenev, L. Tsybeskov, J.-M. Baribeau, and D. J. Lockwood, *Appl. Phys. Lett.* **84**, 1293 (2004).
- ³B. V. Kamenev, E.-K. Lee, H.-Y. Chang, H. Han, H. Grebel, and L. Tsybeskov, *Appl. Phys. Lett.* **89**, 153106 (2006).
- ⁴R. Apetz, L. Vescan, A. Hartmann, C. Dieker, and H. Lüth, *Appl. Phys. Lett.* **66**, 445 (1995).
- ⁵B. V. Kamenev, L. Tsybeskov, J.-M. Baribeau, and D. J. Lockwood, *Phys. Rev. B* **72**, 193306 (2005).
- ⁶C. J. Williams, E. Corbin, M. Jaros, and D. C. Herbert, *Physica B* **254**, 240 (1998).
- ⁷T. Baier, U. Mantz, K. Thonke, R. Sauer, F. Schäffler, and H.-J. Herzog, *Phys. Rev. B* **50**, 15191 (1994).
- ⁸W. Seidel, A. Titkov, J. P. André, P. Voisin, and M. Voos, *Phys. Rev. Lett.* **73**, 2356 (1994).
- ⁹P. P. Paskov, P. O. Holtz, B. Monemar, J. M. Garcia, W. V. Schoenfeld, and P. M. Petroff, *Appl. Phys. Lett.* **77**, 812 (2000).
- ¹⁰G. G. Zegrya and V. A. Kharchenko, *Zh. Eksp. Teor. Fiz.* **101**, 327 (1992) [*Sov. Phys. JETP* **74**, 173 (1992)].
- ¹¹M. I. Dyakonov and V. Y. Kachorovskii, *Phys. Rev. B* **49**, 17130 (1994).
- ¹²H. K. Shin, D. J. Lockwood, and J.-M. Baribeau, *Solid State Commun.* **114**, 505 (2000).
- ¹³P. L. Gourley and J. P. Wolfe, *Phys. Rev. B* **25**, 6338 (1982).
- ¹⁴J. Shah and A. H. Dayem, *Phys. Rev. Lett.* **37**, 861 (1976).
- ¹⁵C. D. Jeffries, *Science* **189**, 955 (1975).
- ¹⁶J. D. Cuthbert, *Phys. Rev. B* **1**, 1552 (1970).
- ¹⁷J. I. Pankove, *Optical Processes in Semiconductors* (Dover, New York, 1975).
- ¹⁸W. F. Brinkman and T. M. Rice, *Phys. Rev. B* **7**, 1508 (1973).
- ¹⁹J. C. Hensel and R. C. Dynes, *Phys. Rev. Lett.* **39**, 969 (1977).
- ²⁰M. E. Msall and J. P. Wolfe, *Phys. Rev. B* **65**, 195205 (2002).
- ²¹E. M. Conwell, *High Field Transport in Semiconductors* (Academic, New York, 1967).
- ²²M. Tajima and S. Ibuka, *J. Appl. Phys.* **84**, 2224 (1998).
- ²³N. Pauc, V. Calvo, J. Eymery, F. Fournel, and N. Magnea, *Opt. Mater.* **27**, 995 (2005).
- ²⁴L. V. Keldysh, *Contemp. Phys.* **27**, 395 (1986).